



***In-vitro* Measurement of Glucose Concentration in Human Blood Plasma Mixed Intralipid Phantom Samples by Using Modulated Ultrasound and Infrared Light**

Anuj Srivastava^{1*}, Md. Koushik Chowdhury¹, Shiru Sharma¹ and Neeraj Sharma¹

¹*School of Biomedical Engineering, Indian Institute of Technology (Banaras Hindu University), Varanasi, Uttar Pradesh-221005, India.*

Authors' contributions

This work was carried out in collaboration between all authors. Author AS designed the experimental study and wrote the investigational protocols. Author MKC performed the Bland Altman plot, Error-Grid and statistical analysis. Authors AS and MKC wrote the first draft of this manuscript. Authors SS and NS supervised the experimental study to ensure accuracy at every step. All authors read and approved the final manuscript.

Article Information

DOI: 10.9734/BBJ/2016/24861

Editor(s):

(1) Chan Yean Yean, Department of Medical Microbiology and Parasitology, School of Medical Sciences, Universiti Sains Malaysia, Malaysia.

Reviewers:

- (1) Elvira Bormusov, The Lloyd Rigler Sleep Apnea Research Laboratory, Unit of Anatomy and Cell Biology, Israel.
 - (2) Monica Souza de Miranda Henriques, Universidade Federal da Paraíba, Brazil.
 - (3) Simon C. H. LAM, The Hong Kong Polytechnic University, Hong Kong, China.
- Complete Peer review History: <http://sciencedomain.org/review-history/13975>

Original Research Article

Received 4th February 2016
Accepted 16th March 2016
Published 1st April 2016

ABSTRACT

Non-invasive blood glucose measurement is one of most innovative domain in Biomedical Engineering. Multiple methodologies have-been introduced over last few decades to fulfil the clinical requirement for non-invasive glucose measurement in human beings, however, without a successful breakthrough. This research article uses modulated ultrasound with infrared light-based technique to study glucose-induced variations in human blood plasma mixed Intralipid™ phantom samples using infrared light of 940 nm and 40 kHz central frequency based ultrasonic transmitter unit. The test uses blood samples of 30 study subjects during oral glucose tolerance test and fasting, postprandial and random stages based blood glucose tests respectively. The result as obtained from oral glucose tolerance tests and fasting, postprandial and random stages blood

*Corresponding author: E-mail: anuj.srivastava100@gmail.com;

glucose tests showed peak amplitude values in Fast Fourier Transform domain varies in corresponding to blood glucose levels in *in-vitro* samples. The Bland Altman plot, Error Grid and statistical analysis represent the potentiality and feasibility of our technique for non-invasive blood glucose measurement.

Keywords: Non-invasive; modulated ultrasound; infrared light, Intralipid™ phantom; blood glucose.

1. INTRODUCTION

Diabetic patients need to monitor their respective blood glucose levels 3 to 4 times per day. Since established techniques necessitate the application skin/finger prick needles, there is a prodigious requirement for continuous, non-invasive techniques [1-4]. In last few decades, numerous techniques have been explored including Near Infrared Spectroscopy [4,5], Infrared Spectroscopy [4,5], Raman Spectroscopy [4,5], Polarization Spectroscopy [4,5], Photo Acoustic Techniques [4,5], Optical Coherence Tomography (OCT) [4,5]. However, various techniques even after their exhaustive exploration suffer from certain difficulties, impeding their revolution in this research field. Simultaneously, our knowledge about the different characteristics of tissue optical properties has improved [4-6], moderately due to *in-vitro* experimentations [5] that lead to the growth of various types of tissue phantom models. Hence, our present study conducted for measuring glucose concentration in Human Blood Plasma mixed Intralipid Phantom Samples by using indigenously developed modulated ultrasound and infrared light based technique.

2. MATERIALS AND METHODOLOGY FOR *In-vitro* BLOOD GLUCOSE MEASUREMENT

Zhu et al. [7] and Zhu et al. [8] introduced a methodology of using ultrasound modulated optical technique for blood glucose-concentration determinations. Their *in-vitro* studies based upon the measurement of ultrasonic modulation depth through ultrasound modulated scattered light.

They introduced the application of ultrasound with light modulation techniques [7,8]. However, in this present study, the modulated ultrasound exhibits vibrations inside the *in-vitro* phantom samples and the infrared light measures those glucose molecule specific vibrations for glucose concentration measurement.

When ultrasonic waves with amplitude modulation characteristics propagates through the *in-vitro* phantom samples, the molecules

present within that medium experiences vibrations due to the impact of pressure exhibited by the amplitude modulating ultrasonic waves. The inherent characteristics of molecules existing within that *in-vitro* sample medium effect the compressibility factor of the medium. The physical properties of the molecules existing within that *in-vitro* medium exhibit the vital role. The degree of influence over larger molecules are larger and vice-versa [9-18].

Henceforth, the vibration generated in that *in-vitro* sample medium hinge on (a) its three dimensional organisations, (b) inherent characteristics of the *in-vitro* sample molecules, (c) nature and characteristics of the amplitude modulated ultrasonic waves [9-15].

The ultrasonic standing wave pressure amplitude possesses maximum and minimum values two times over the space of one unit wavelength. Inside the ultrasound-propagating segment, the molecules attain area definite ultrasonic potential energy owing to their existence in that particular domain. The suspended molecules initiate to travel and gather adjacently to the area of low ultrasonic potential energy. Generally, these areas locate nearby to the pressure nodes, spaced from each other by half a wavelength distances [9-18].

Afterwards, when the molecular physical characteristics is lesser than the wavelength of the transmitting ultrasound within the *in-vitro* phantom samples, the foremost radiation force (F_r) applied over the molecular volume (V_c), located by space (z) starting from the node of pressure is measured from the molecular ultrasonic potential energy based gradient values and scientifically represented as:

$$F_r = - \left[\frac{\pi P_o^2 V_c \beta_w}{2\lambda} \right] \cdot \phi(\beta, \rho) \cdot \sin(4\pi z/\lambda) \quad (1)$$

In this paper, the (P_o) signifies ultrasonic peak amplitude. (λ) stands for wavelength of ultrasound in that *in-vitro* sample medium. The compressibility of the medium have been denoted as (β_w), and scientifically represented [12,13] as:

$$\phi(\beta, \rho) = \left[\frac{5\rho_c - 2\rho_w}{2\rho_c + \rho_w} - \left(\frac{\beta_c}{\beta_w} \right) \right] \quad (2)$$

Here, the molecular compressibility have been denoted as (β_c). Further, the symbols (ρ_c) and (ρ_w) represents molecular density and suspending segment density respectively [12,13].

To quantify the specific absorption (**A**) characteristics of the glucose molecules at a particular light wave number (**v**), the famous Lambert-Beer law has been introduced and scientifically represented as:

$$A(v) = -\log I(v)/I_0(v) \quad (3)$$

Herein, the (**I₀**) stands for the surrounding area light intensity and (**I**) signifies the particular light intensity at specific wave number (**v**) of the in-vitro sample measurements [12,13].

Henceforth, as per Urban et al. [19] and Silva et al. [20], we attain the advantage of beam formation at the specific frequency of ultrasound for focussing the radiation force of energy towards the in-vitro optical phantom sample mediums. This generates vibration characteristics at lower frequencies, for which the displacements are adequate enough for measurement with the aid of infrared red light based techniques accordingly.

In this reported work, the entire observed signal undergoes signal analysis through the signal processing toolbox of MATLAB. The peak amplitude in the FFT (Fast Fourier Transform) domain were monitored here to extract glucose concentration based embedded information from the observed signals as acquired from the in-vitro samples.

Our methodology based Instrumental prototype descriptions:

Firstly, it contains the explanation about ultrasound transmitter, receiver, and LED (Light Emitting Diode) light wavelength range tracked by the descriptions of our methodology based Instrumental prototype.

2.1 Selection of Ultrasound Frequency

In Biomedical Engineering domain, the ultrasound transmitter of 40 kHz provides significant help in improving (a) fibrinolysis [20-26], (b) skin-tissue infiltrations [20-26], (c) clot removal processes [20-26], (d) thrombolysis [20-26], (e) remedial of cuts and wounds [20-26]. In our application, we have introduced 40 kHz

ultrasonic transmitter to generate modulated ultrasonic pressure waves for generating vibration inside the in-vitro samples. Moreover, (a) ease of use, (b) clinically safe and acceptable [20-26], (c) small heating effects [20-26], and, (d) economical rate of 40 kHz ultrasound transmitter has driven us for its usage in our application.

2.2 Selection of Light Wavelength

Human blood is a liquid connective tissue and consists of multiple constituents within it. Moreover, glucose induces very feeble signals. The criteria for light wavelength selection must be rigid to overwhelm this typical fact.

As per Konig [27], the light wavelength extending from 600 nm to 1100 nm often called as the "Optical Window" of the living skin-tissue cells. Further, the oxy-haemoglobin and deoxy-haemoglobin exhibits less absorption profile in the light wavelength bands extending from 900 nm to 1100 nm correspondingly. Hence, blood oxygenation induced changes will be lower in this particular band.

Khalil [28] and Khalil [29] published that the glucose molecule shows peak absorption characteristics at 939 nm that is very close to 940 nm. Furthermore, selecting wavelength range in between "Optical Window" zone where, water, oxy-haemoglobin and deoxy-haemoglobin shows less absorption interferences will be significant [30].

Henceforth, we have selected 940 nm based infrared light emitting diode of Roithner-Laser-Technik, Vienna, Austria for our application.

2.3 Fabricated Prototype Descriptions

The Fig. 1 presents the block diagram of our technique based prototype (MUS-IR) unit for measuring blood glucose levels in the Human Blood Plasma mixed Intralipid Phantom based *in-vitro* Samples.

Our method utilizes modulated ultrasound and infrared light based optical technique for in-vitro measurement of blood glucose levels. The modulating signal unit provides modulating sine wave signals. The Carrier wave unit provides carrier wave signals. Both this signals serves as an input to the modulator unit. The modulator unit produces amplitude modulated sine wave signals to the ultrasound transmitter unit. The Ultrasound transmitter unit produces ultrasonic amplitude modulated sine waves to the sample holder unit.

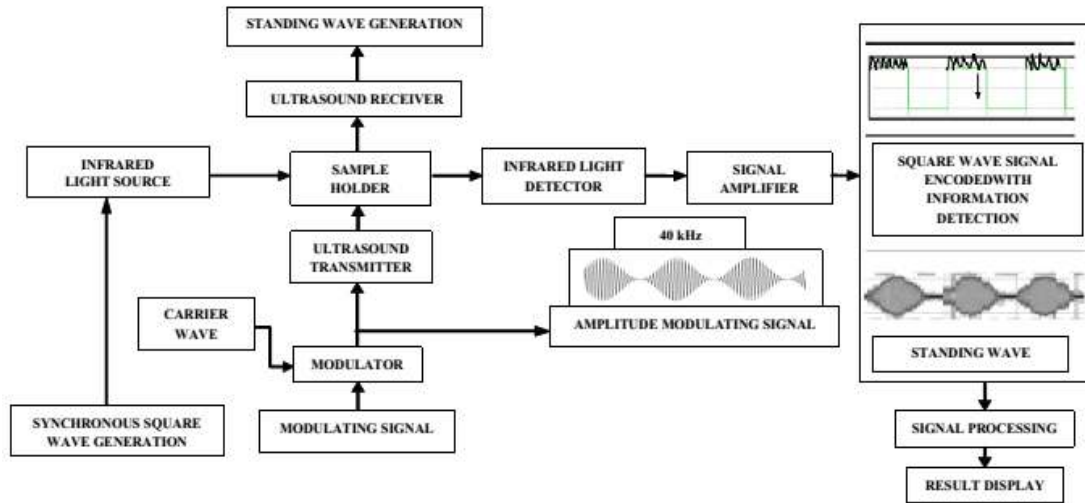


Fig. 1. Block diagram of our technique based prototype (MUS-IR) unit

The amplitude modulated ultrasonic waves excites the in-vitro samples, as a result different constituent molecules vibrates at their specific response frequency depending upon their weight, shape, size, and properties of the medium in which they are present [12-18].

The ultrasound receiver unit cross checks the pattern of amplitude-modulated signal waves as generated by ultrasound transmitter unit as shown in the oscilloscope monitor block in figure 1 respectively. The synchronous square wave generations are-provided to the Infrared light source unit, to deliver square wave pulses to the sample holder unit. Further, the specific vibrations produced due to amplitude modulated ultrasonic waves are detected using the infrared light and detector unit. The amplified output response signal is in the form of synchronous square wave signals as shown in the oscilloscope monitor block of Fig. 1, which carries encoded information about the concentration of different constituent molecules. This modulated light response signal as collected using Infrared light detector are suitably processed to extract the information of about the blood glucose concentration and then the display unit shows the results in mg/dl unit.

3. STUDY SUBJECTS

In total thirty adult subjects (eighteen males and twelve females) participated in this OGTT (Oral Glucose Tolerance Test) based first phase of clinical study. Here, the study subjects are

healthy, normal (age = 27.3 ± 4.6 years, height = 163 ± 3.5 cm, weight = 75 ± 4.0 kg human beings. Further, in Second phase, thirty more adults inclusive of healthy and diabetic subjects (twenty-one males and nine females) are recruited for measuring blood glucose levels during their fasting stage, postprandial stage and random stages respectively. Here, the study subjects includes healthy normal and diabetic subjects of age = 43 ± 15 years, height = 170 ± 5.5 cm, and weight = 76 ± 5.5 kg. The clinical studies reported here are in accordance with the standard ethical procedures and performed with the informed consent of all the respective study subjects. The Ethical committee of Institute of Medical Sciences, Banaras Hindu University, Varanasi, approved the clinical study.

4. SAMPLE PREPARATION

Researchers regularly examine the NIR (Near Infra-Red) glucose concentration in in-vitro samples for preliminary investigations before proceeding with in-vivo determinations. In this aspect, Intralipid™ based optical phantoms utilized here to validate various investigational objectives. Intralipid suspension main constituents are **soya bean oil, lecithin, glycerin, and water** [31,32]. Commercially, available as Intralipid™10% (**10% lipid indicates 10 g of lipid per 100 ml of suspension**) and Intralipid™20%. The Table 1 depicts the constituents of 10% Intralipid™ in a 500 ml bottle according to the manufacturer are:

Table 1. 10% Intralipid™ suspension constituents [31,32]

10% Intralipid™ suspension constituents		
Soybean oil	50 g	53.94 ml
Lecithin from egg yolk	6 g	5.82 ml
Glycerin (C ₃ H ₈ O ₃)	11.25 g	8.92 ml
Water (H ₂ O)	430.5 g	431.33 ml
Total Volume	497.75 g	500 ml

For preparing human blood plasma samples, we have collected 5 ml of whole blood samples from the study subjects in EDTA (Ethylene Di-amine Tetra Acetic Acid)-treated blood collecting vials. Afterwards, all the collected samples undergoes centrifugation process for 10 to 15 minutes. The centrifugation process produces supernatant fluid portion, which is termed as blood plasma [34]. In our proposed work, we have added 1 ml of blood plasma sample with the 3 ml of 10% Intralipid™ tissue phantom solution to resemble blood-tissue-phantom medium complex.

5. CALIBRATION

The peak amplitude in the FFT domain corresponds to the blood glucose concentration in Human Blood Plasma mixed Intralipid Phantom Samples. The product of Calibration Factor (CF) with the peak amplitude (mV) in the FFT domain yields predicted blood glucose concentration in mg/dl and scientifically expressed here as:

$$V_{peak} \times CF = PBGL \quad (4)$$

Where, V_{peak} stands for peak voltage amplitude (mV) in FFT domain, CF stands for Calibration Factor, and PBGL refers to Predicted Blood Glucose Level in mg/dl.

6. EXPERIMENTAL PROTOCOL

In this present work, we have performed our clinical study in two phases that includes oral glucose tolerance test and fasting, postprandial, random stage based blood glucose test respectively to validate the clinical relationship amid the invasive methodology and non-invasive methodology applied here.

In first phase, the oral glucose tolerance tests were-conducted in the morning over 30 healthy subjects after 10-12 hour overnight fasting period. The period of each tests has been 2 hour and 30 minutes inclusive of baseline monitoring

after 75-gram glucose solution intake. Both the reference and predicted blood glucose levels were-recorded every 30 minutes from right and left hand respectively. For reference and predicted results, we have performed blood glucose measurement using established GOD/POD (Glucose Oxidase/ Peroxidase) method [33] and by our proposed technique based MUS-IR unit respectively. During the course of the tests, all the study subjects were-instructed to remain static to reduce the influence of motion artefacts. Further, any kind of food or liquid intake has been-prohibited.

During the second phase, we have performed Blood glucose level tests over healthy normal and diabetic subjects during fasting stage, postprandial stage and random stage respectively. Further, all the blood glucose measurements reported in this present work was-performed under the controlled conditions of temperature and humidity respectively.

7. RESULTS AND DISCUSSION

The present paper describes OGTT (Oral Glucose Tolerance Test) and Fasting, Postprandial and Random stage based experiments as performed by mixing human blood plasma with Intralipid™ phantom samples during the pilot study. The OGTT helps in tracking the effect of 75 gm/100 ml on healthy individual glucose metabolism in-between the scheduled periods [2-4]. The Fig. 2 describes the pattern of OGTT from the Healthy Subject 1 as obtained from the healthy normal subject during our pilot study.

The fasting stage Blood Glucose Level defines a physiological condition, when the concerned individual has been restricted from the intake of any food items up to 8 to 10 hours [2-4].

The Postprandial stage Blood Glucose Level defines the physiological conditions, when the concerned individual has taken food diet two hours prior to the blood examination [2-4].

The Random stage Blood Glucose Level defines the physiological conditions, when the concerned individual has taken food diet anytime during daytime and not in fasting mode [2-4].

The Fig. 3 describes the fasting, postprandial and random stages of the healthy normal subject 1 and a diabetic subject 5 during our pilot study.

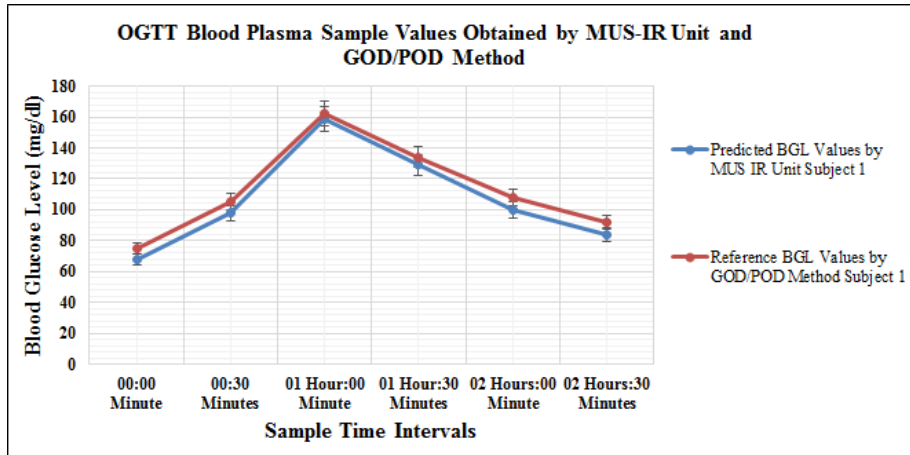


Fig. 2. OGTT pattern as obtained from the healthy subject 1 during our pilot study; error bar indicates ± 5 percentage errors

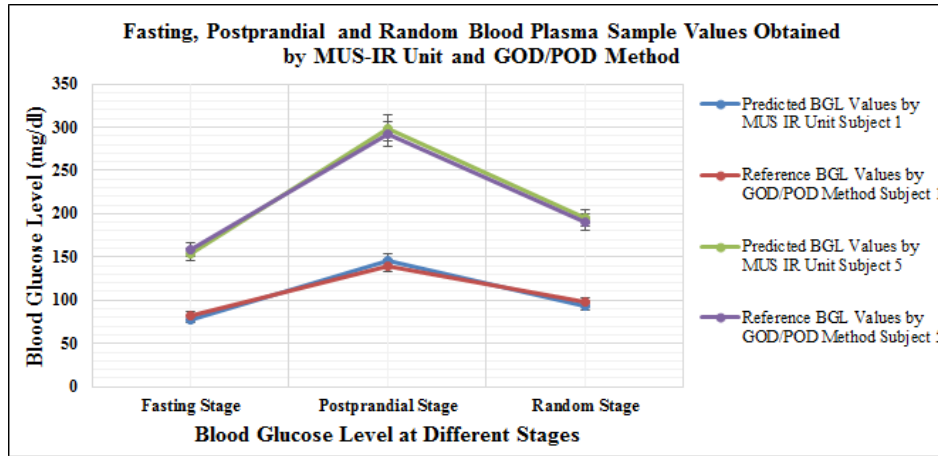


Fig. 3. Fasting, postprandial and random stage based blood glucose levels of subject 1 and diabetic subject 5 as obtained during our pilot study; error bar indicates ± 5 percentage errors

Further, in this section, we have performed Clarke and Parkes Error Grid analysis, Bland Altman plot analysis and statistical analysis for the result investigation purposes.

7.1 Error Grid Analysis

In general, the Clarke and Parkes error grid analysis judgements assess the clinical significance of the differences between reference and predicted results. In both the error grid analysis results in A and B zones are clinically significant. Further, results in C to E zones are clinically insignificant respectively [35-42].

The Figs. 4(a), 4(b) and 5(a), 5(b) depicts Clarke, Parkes Error Grid Analysis of the blood glucose

data pair sets inclusive of reference, and predicted readings as obtained during OGTT and fasting, postprandial and random stage based clinical studies respectively. For OGTT based study, the Clarke Error Grid analysis shows that the percentage of the total data pairs (180) falling in zones A, B, C, D, and E are 83.34% (150 data pairs), 13.33% (24 data pairs), 00.00% (00 data pairs), 03.33% (06 data pairs), and 00.00% (00 data pairs), respectively. Further, the Parkes Error Grid analysis shows that the percentage of the total data pairs (180) falling in zones A, B, C, D, and E are 83.34% (150 data pairs), 13.89% (25 data pairs), 02.77% (05 data pairs), 00.00% (00 data pairs), and 00.00% (00 data pairs), respectively. Very few results occupy medically insignificant C and D zone respectively.

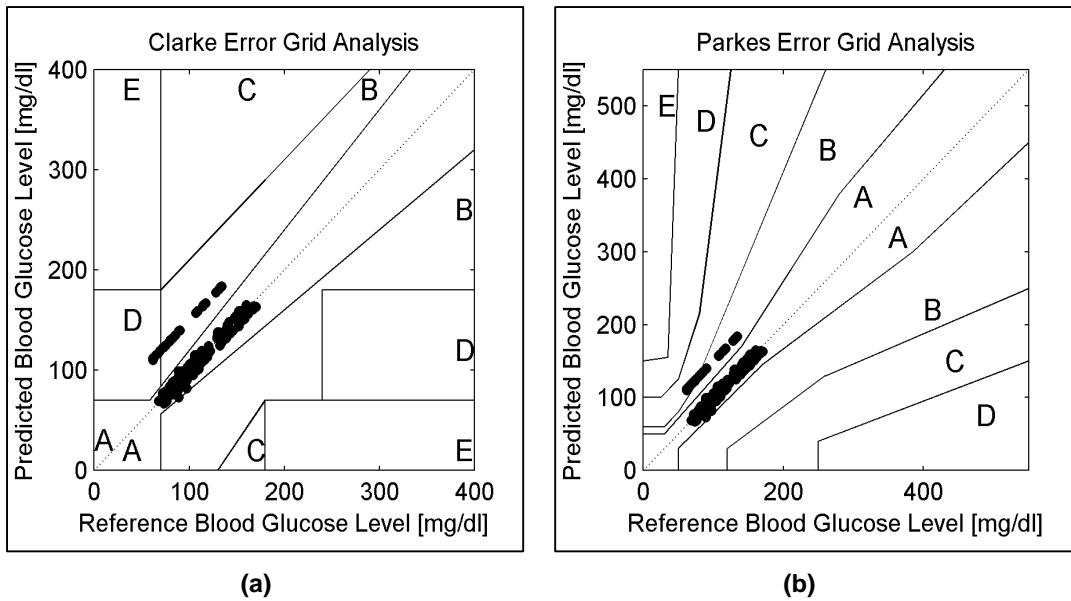


Fig. 4. The (a) Clarke, (b) Parkes error grid analysis of the OGTT based reference and predicted blood glucose measurements

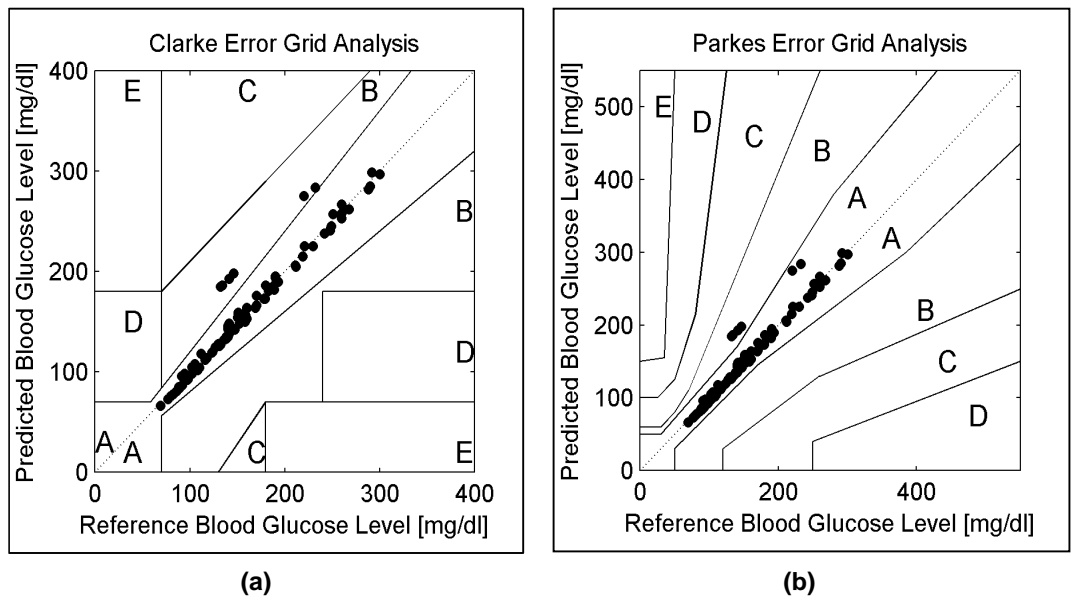


Fig. 5. The (a) Clarke, (b) Parkes error grid analysis of the fasting-postprandial-random stage based blood glucose measurements

For fasting, postprandial and random based study, the Clarke Error Grid analysis shows that the percentage of the total data pairs (90) falling in zones A, B, C, D, and E are 93.34% (84 data pairs), 06.66% (06 data pairs), 00.00% (00 data pairs), 00.00% (00 data pairs), and 00.00% (00 data pairs), respectively. Further, the Parkes Error Grid analysis shows that the percentage of the total data pairs (90) falling in zones A, B, C,

D, and E are 95.56% (86 data pairs), 04.44% (04 data pairs), 00.00% (00 data pairs), 00.00% (00 data pairs), and 00.00% (00 data pairs), respectively. Hence, the Error Grid Analysis depicts that maximum data pairs of the estimations are in medically significant and acceptable A and B zones respectively. Here, none of the results occupies medically insignificant C to E zone respectively.

7.2 Bland Altman Plot Based Analysis

The Bland-Altman plot (difference plot) represents the graph-based approach to equate two measurement methods. This graphical approach depicts the plotting of the differences between the two methods versus the mean of the two methods. The Bland-Altman plot (parametric method) signifies the connection between the differences and the mean of two methods to find systemic biases [43-45]. Here, the two measurement methods indicates the results as obtained from Reference (GOD/POD) and Predicted (our proposed method) methods respectively. As per Bland et al. [44] and Bland et al. [45], in this present work, the Bland-Altman Plot with the mean of the same two methods on x-axis and the differences of the two methods on y-axis has-been-plotted [43]. For validating successful clinical study, the bias had to be ≤ 15

mg/dl (null hypothesis) [46,47]. In this present work, the testing of this hypothesis performed at overall blood glucose levels as obtained during our OGTT and fasting, postprandial and random stages based blood glucose measurements. Including OGTT and fasting, postprandial and random stage based paired data sets; the overall Reference blood-glucose range has been 62-300 mg/dl.

In Fig. 6(a) and 6(b), the dotted red line represents the line of equality (difference = 0). The horizontal line (dash blue line) and horizontal dotted green lines in Fig. 6(a), (b) depicts the mean difference line and 95% confidence interval of mean differences line respectively. This horizontal dotted green lines show the magnitude of systemic difference. If the line of equality does not present in this interval, it indicates statistically significant systemic difference exists.

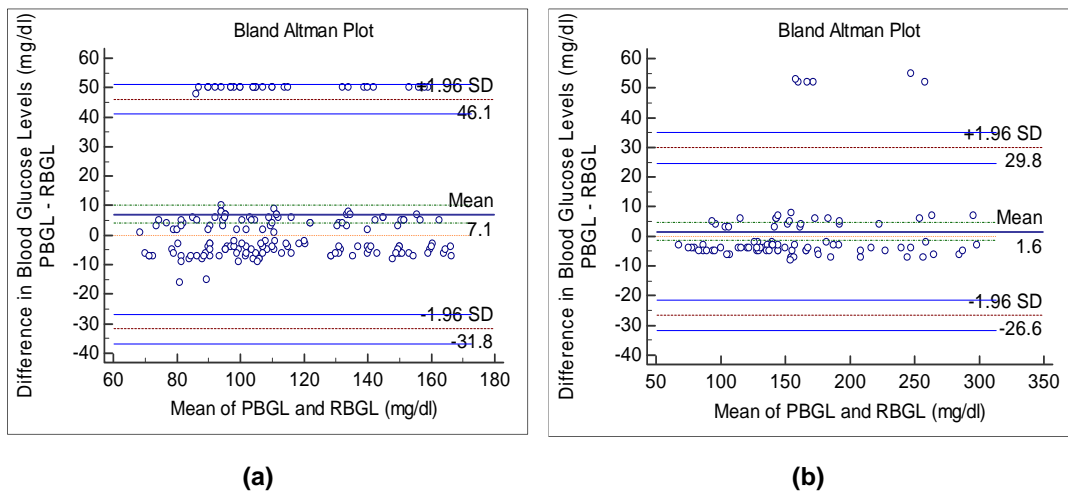


Fig. 6. Bland Altman plot based analysis of (a) the OGTT based measurements and (b) fasting, postprandial and random stage based measurement of blood glucose levels respectively

Table 2. Bland-Altman plot based analysis of both the OGTT and fasting-postprandial-random stages based blood glucose measurement

Bland-Altman Plot based analysis		
Method A (Predicted method)	PBGL (mg/dl)	
Method B (Reference method)	RBGL (mg/dl)	
Differences in mg/dl		
Sample size (n number of data pairs)	180 data pairs of OGTT	90 data pairs of Fasting-postprandial-random stages
Bias	7.1222 mg/dl	1.6333 mg/dl
95% CI (Confidence interval)	4.1997 to 10.0447 mg/dl	-1.3807 to 4.6474 mg/dl
P-value	<0.0001	<0.0001
Standard deviation	19.8699 mg/dl	14.3906 mg/dl

The limits of agreements (dotted brown lines), that states the mean difference ± 1.96 times the SD (Standard Deviation) of the differences respectively.

The Table 2 depicts the result of the Bland-Altman analysis for paired data sets, corresponding to Predicted and Reference blood glucose levels. In order to compare the Predicted BGL method with the standard Reference BGL measurement method, a Bland-Altman plot based analysis performed on all paired glucose values and utilized to measure bias of glucose overall the range of values. The measured bias in mg/dl at the overall glucose levels during OGTT was found to be (95% Confidence Interval) 7.1222 (4.1997 to 10.0447). Further, the measured bias in mg/dl at the overall glucose levels during fasting, postprandial and random stage based tests was found to be (95% Confidence Interval) 1.6333 (-1.3807 to 4.6474). Based on these outcome, the null hypothesis (bias > 15 mg/dl) [47] has been rejected and both sided P-value (< 0.0001) less than the conventional 0.05 significance level implies that the bias of the overall blood glucose measurement has been statistically significant. The Standard Deviation (SD) in mg/dl of the OGTT and fasting, postprandial and random stage based tests, the blood glucose-measurement differences as per Bland-Altman plot based analysis has been ± 198699 mg/dl and ± 14.3906 mg/dl respectively.

As per Clarke et al. [36] and Wentholt et al. [48], the positive and negative bias signifies overestimation and underestimation of actual blood glucose levels respectively. In this present work, negative bias signifies underestimation of Reference Blood Glucose Levels by our proposed technique based Predicted Blood Glucose Levels. Hence, the Bland-Altman plot analysis depicts statistical significance of our overall blood glucose-measurement during clinical studies. This phenomenon directs towards the capability of our technique based prototype unit to perform blood glucose measurement in human subjects.

7.3 Overall Statistical Analysis

The Table 3 depicts our performance assessment values as acquired during OGTT, fasting, postprandial and random stage based blood glucose measurement results comparison with other Non-invasive Techniques, and Continuous Glucose Monitoring System(s) (CGMS) based published data ranges. The

OGTT analysis based performance metrics errors such as MAE (Mean Absolute Error), MdAE (Median Absolute Error), and RMSE (Root Mean Squared Error) values were 12.77 mg/dl, 06.00 mg/dl, and 21.06 mg/dl respectively. Further, fasting, postprandial and random stage centred blood glucose analysis based performance metrics errors such as MAE (Mean Absolute Error), MdAE (Median Absolute Error), and RMSE (Root Mean Squared Error) values were 07.88 mg/dl, 05.00 mg/dl, and 14.40 mg/dl respectively.

Similarly, the OGTT analysis based performance metrics based percentage errors such as Percentage-MARE (Percentage of Mean Absolute Relative Error), and Percentage-MdARE (Percentage of Median Absolute Relative Error) values were 13.89%, and 05.14% respectively. Further, fasting, postprandial and random stage centred blood glucose analysis based performance metrics based percentage errors such as Percentage-MARE (Percentage of Mean Absolute Relative Error), and Percentage-MdARE (Percentage of Median Absolute Relative Error) values were 05.20%, and 03.24% respectively.

Correspondingly, the SEP (Standard Error of Prediction) and Pearson's Correlation Coefficient (r) values of OGTT based analysis were 18.87 mg/dl and 0.73 respectively. Further, the SEP (Standard Error of Prediction) and Pearson's Correlation Coefficient (r) values of fasting, postprandial and random stage centred blood glucose-analysis were 14.46 mg/dl and 0.97 respectively. Further, as depicted from Table 3, the output results obtained by our proposed technique are better than or comparable with other non-invasive blood glucose monitoring techniques. Further, its accuracy levels are also akin with other commercially existing Continuous Glucose Monitoring System(s). Hence, all these overlaid accuracy measures based statistical analysis depicts the strong promising aspect of our technique for non-invasive blood glucose measurement in the human subjects.

Further, the Table 4 depicts the statistical parameters for error prediction during OGTT. The SEP, RMSE value extends from 11.56 mg/dl to 17.85 mg/dl, and 20.98 mg/dl to 21.01 mg/dl respectively. The MAE and MdAE value ranges from 12.57 mg/dl to 13.14 mg/dl and 5.00 mg/dl to 7.00 mg/dl respectively. Further, the %MARE and %MdARE values extends from 9.80% to 18.43% and 3.64% to 7.62% respectively.

Table 3. Performance metrics based statistical analysis

Statistical parameters for error prediction	Assessment values		Published data ranges of other developing noninvasive blood glucose monitoring techniques [47-76]
	OGTT based blood glucose measurement results	Fasting-postprandial-random stage based blood glucose measurement results	
Pearson correlation coefficient (R-Value)	0.73	0.97	00.49 to 00.95
Standard error of prediction (SEP)	18.87 mg/dl	14.46 mg/dl	07.10 to 35.30 mg/dl
Mean absolute error (MAE)	12.77 mg/dl	7.88 mg/dl	07.00 to 30.00 mg/dl
Median absolute error (MdAE)	6.00 mg/dl	5.00 mg/dl	10.40 to 19.10 mg/dl
Root mean squared error (RMSE)	21.06 mg/dl	14.40 mg/dl	25.00 to 46.00 mg/dl
Percentage of mean absolute relative error (% MARE)	13.89%	5.20%	08.60 to 40.80%
Percentage of median absolute relative error (% MdARE)	5.14%	3.24%	07.70 to 30.00%

Table 4. Statistical parameters for Error prediction during OGTT

Statistical parameters for error prediction	Assessment Values of OGTT					
	00:00 minute	00:30 minutes	01 hour:00 minute	01 hour:30 minutes	02 hours:00 minute	02 hours:30 minutes
Standard error of prediction (SEP)	13.98 mg/dl	11.56 mg/dl	14.89 mg/dl	16.65 mg/dl	12.52 mg/dl	17.85 mg/dl
Root mean squared error (RMSE)	21.01 mg/dl	21.05 mg/dl	20.98 mg/dl	21.01 mg/dl	21.08 mg/dl	21.18 mg/dl
Mean absolute error (MAE)	13.14 mg/dl	12.74 mg/dl	12.60 mg/dl	12.76 mg/dl	12.80 mg/dl	12.57 mg/dl
Median absolute error (MdAE)	7.00 mg/dl	5.50 mg/dl	6.00 mg/dl	6.00 mg/dl	6.00 mg/dl	5.00 mg/dl
Percentage of mean absolute relative error (% MARE)	18.43%	14.92%	9.80%	9.97%	14.31%	15.89%
Percentage of median absolute relative error (% MdARE)	7.62%	5.55%	3.64%	4.03%	5.58%	5.47%

Table 5. Statistical parameters for error prediction during fasting, postprandial and random stages

Statistical parameters for error prediction	Assessment values at different stages		
	Fasting stage	Postprandial stage	Random stage
Standard Error of Prediction (SEP)	14.69 mg/dl	15.07 mg/dl	14.54 mg/dl
Root Mean Squared Error (RMSE)	14.22 mg/dl	14.68 mg/dl	14.32 mg/dl
Mean Absolute Error (MAE)	7.47 mg/dl	8.13 mg/dl	8.03 mg/dl
Median Absolute Error (MdAE)	4.50 mg/dl	5.00 mg/dl	5.00 mg/dl
Percentage of Mean Absolute Relative Error (% MARE)	5.99%	3.88%	5.73%
Percentage of Median Absolute Relative Error (% MdARE)	3.56%	2.39%	3.45%

The Table 5 depicts the statistical parameters for error prediction during fasting, postprandial and random stages. The SEP, RMSE value extends from 14.54 mg/dl to 15.07 mg/dl, and 14.22 mg/dl to 14.68 mg/dl respectively. The MAE and MdAE

value ranges from 7.47 mg/dl to 8.13 mg/dl and 4.50 mg/dl to 5.00 mg/dl respectively. Further, the %MARE and %MdARE values extends from 3.88% to 5.99% and 2.39% to 3.56% respectively.

8. CONCLUSION

In this paper, we depicted the feasibility of the modulated ultrasound and infrared light based technique for blood glucose measurement in in-vitro intralipid mixed blood samples. The in-vitro results produce promising results.

Moreover, the Error grid analysis, Bland Altman plot, and Statistical Analysis depicts the acceptable efficiency of the proposed technique in measuring blood glucose levels in in-vitro samples as obtained during OGTT and fasting, postprandial and random stages respectively.

Henceforth, our proposed technique is reliable to measure blood glucose concentration in Intralipid™ and human blood plasma mixed samples. Positively, this technique will be helpful in developing non-invasive glucometer in near future.

CONSENT

Informed consent was obtained from all individual participants included in the study.

ETHICAL APPROVAL

All procedures performed in studies involving human participants were in accordance with the ethical standards of the institutional and/or national research committee and with the 1964 Helsinki declaration and its later amendments or comparable ethical standards.

This article does not contain any studies with animals performed by any of the authors.

COMPETING INTERESTS

Authors have declared that no competing interests exist.

REFERENCES

1. International Diabetes Federation. IDF Diabetes Atlas 6th edn. Brussels, Belgium: International diabetes Federation; 2013. Available:<http://www.idf.org/diabetesatlas> (22/01/2016)
2. Peter J. Watkins. ABC of Diabetes. (Fifth Edition), London: BMJ Books; 2003.
3. Available:<http://diabetes.webmd.com/> (23/01/2016)
4. Tuchin VV, (ed.). Handbook of optical sensing of glucose in biological fluids and tissues. CRC Press, Taylor & Francis Group, London; 2009.
5. Tura A, Maran A, Pacini G. Non-invasive glucose monitoring: Assessment of technologies and devices according to quantitative criteria. Diabetes Research and Clinical Practice. 2007;77:16-40.
6. "Special issue on non-invasive glucose monitoring with optical technique", IEEE Leos Newsletter; 1998.
7. Zhu L, Lin J, Lin B, Li H. Noninvasive blood glucose measurement by ultrasound-modulated optical technique. Chinese Optical Letters. 2013;11(2): 0217011-15.
8. Zhu Lili, Lin Jieqing, Xie Wenming and Li Hui. New optical method for noninvasive blood glucose measurement by optical ultrasonic modulation. Proc. SPIE 7845, Optics in Health Care and Biomedical Optics IV. 2010;784525.
9. Haar G Ter, Wyard SJ. Blood cell banding in ultrasonic standing wave fields: A physical analysis. Ultrasound in Medicine and Biology. 1978;4(2):111-123.
10. Chowdhury Md Koushik, Srivastava Anuj, Sharma Shiru, Sharma Neeraj. The potential application of amplitude modulated ultrasound with Infrared Technique for blood glucose level determination in non invasive manner. Biomedical and Pharmacology Journal. 2014;7(1):195-206.
11. Chowdhury Md Koushik, Srivastava Anuj, Sharma Shiru, Sharma Neeraj. Five days daily sessions of noninvasive blood glucose level predictions based on amplitude modulated ultrasound and infrared technique over a healthy and diabetic subject'. IOSR-Journal of Electrical and Electronics Engineering. 2014;5(Ver. IV):34-41.
12. Radel S, Brandstetter M, Lendl B. Observation of particles manipulated by ultrasound in close proximity to a cone-shaped infrared spectroscopy probe. Ultrasonics. 2010;50:240–246.
13. Coakley W Terence. Ultrasonic separations in analytical biotechnology. Trends in Biotechnology. 1997;506-511.
14. King LV. On the acoustic radiation pressure on spheres. Proceedings of the Royal Society of London. 1934;212–240. A147.
15. Yosioka K, Kawasima Y. Acoustic radiation pressure on a compressible sphere. Acustica. 1955;5:167–173.

16. Petersson F, Nilsson A, Holm C, Jonsson H, Laurella T. Separation of lipids from blood utilizing ultrasonic standing waves in microfluidic channels. *The Analyst*, The Royal Society of Chemistry. 2004;129:938-943.
DOI: 10.1039/b409139f
17. Chowdhury Md K, Srivastava A, Sharma N, Sharma S. The influence of blood glucose level upon the transport of light in diabetic and non-diabetic subjects. *International Journal of Biomedical and Advance Research*. 2013;4(5):306-316.
DOI: 10.7439/ijbar.v4i5.357
18. Srivastava A, Chowdhury Md K, Sharma S, Sharma N. Optical clearance effect determination of glucose by near infrared technique: An experimental study using an intralipid based tissue phantom. *International Journal of Advances in Engineering & Technology (IJAET)*. 2013;6(3):1097-1108.
19. Urban MW, Fatemi M, Greenleaf JF. Modulation of ultrasound to produce multifrequency radiation force. *Acoustical Society of America*. 2010;1228–38.
20. Urban MW, Silva GT, Fatemi M, Greenleaf JF. Multifrequency vibroacoustography. *IEEE Trans. Med. Imaging*. 2006;25: 1284–95.
21. Mak SY. Wave experiments using low-cost 40 kHz ultrasonic transducers, *Physical Education*. IOP publishing Ltd. 2003;38(5): 441-46.
22. Greenslade TB. Experiments with ultrasonic transducers, *Physical Teacher*. 1994;32:392-397.
23. Suchkova V, Farhan N, Siddiqi, Edwin L, Carstensen, Diane Dalecki, Sally Child, Charles W. Francis. Enhancement of fibrinolysis with 40-kHz ultrasound. *Circulation*. 1998;98:1030-1035.
24. Birnbaum Y. Noninvasive *in vivo* clot dissolution without a thrombolytic drug recanalization of thrombosed ilio femoral arteries by transcutaneous ultrasound combined with intravenous infusion of micro bubbles. *Circulation*. 1998;97:130-134.
25. Suchkova VN, Baggs RB, Francis CW. Effect of 40-kHz ultrasound on acute thrombotic ischemia in a rabbit femoral artery thrombosis model enhancement of thrombolysis and improvement in capillary muscle perfusion. *Circulation*. 2000;101: 2296-2301.
26. Voigt J, Wendelken M, Driver V, Alvarez OM. Low-frequency ultrasound (20-40) kHz as an adjunctive therapy for chronic wound healing: A systematic review of the literature and meta-analysis of eight randomized controlled trials. *Int J Low Extrem Wounds*. 2012;11(1):69.
27. Konig K. Multiphoton microscopy in life sciences. *Journal of Microscopy*. 2004; 200(2):83-104.
28. Khalil OS. Non-invasive glucose measurement technologies: An update from 1999 to the dawn of the new millennium. *Diabetes Technology and Therapeutics*. 2004;6(5):660–97.
29. Khalil OS. Spectroscopic and clinical aspects of noninvasive glucose measurements. *Clin. Chem*. 1999;45:165-77.
30. Tenhunen J, Kopola H, Myllyla R. Non-invasive glucose measurement based on selective near infrared absorption: requirements on instrumentation and special range. *Measurement*. 1998;24: 173–177.
31. Staveren HGV, Moes CJM, Marle J Van, Prah SA, Gemert MJC van. Light scattering in Intralipid-10% in the wavelength range of 400-1100 nanometers. *Applied Optics*. 1991;30: 4507-4514.
32. Flock ST, Jacques SL, Wilson BC, Star WM, Gemert MJC Van. Optical Properties of Intralipid: A phantom medium for light propagation studies. *Lasers in Surgery and Medicine*. 1992;12:510-519.
33. Trinder P. *Ann. Clin. Biochem*. 1969;6:24.
34. Raghu. *Practical biochemistry for medical students*. Jaypee Brother Publishers; 2003.
35. Cox DJ, Clarke WL, Frederick L Gonder, Pohl S, Hoover C, Snyder A, Zimelman L, Carter WR, Bobbitt S, Pennebaker J. Accuracy of perceiving blood glucose in IDDM. *Diabetes Care*. 1985;8(6):529–536.
36. Clarke WL, Frederick L, Gonder A, Carter W, Pohl SL. Evaluating clinical accuracy of systems for self-monitoring of blood glucose. *Diabetes Care*. 1987;10(5):622–628.
37. Kovatchev BP. Evaluating the accuracy of continuous glucose monitoring sensors. *Diabetes Care*. 2004;27(8):1922-28.
38. Maran A. Continuous subcutaneous glucose monitoring in diabetic patients. *Diabetes Care*. 2002;25(2):347-52.
39. Klonoff DC. Continuous Glucose Monitoring, Roadmap for 21st century

- diabetes therapy. *Diabetes Care*. 2005;28:1231-39.
40. Guevara E, Gonzalez FJ. Joint optical-electrical technique for noninvasive glucose monitoring. *REVISTA MEXICANA DE FISICA*. 2010;56(5):430-434.
 41. Parkes JL, Slatin SL, Pardo S, Ginsberg BH. A new consensus error grid to evaluate the clinical significance of inaccuracies in the measurement of blood glucose. *Diabetes Care*. 2000;23(8):1143–1148.
 42. Pftzner A, Klonoff DC, Scott P, Parkes JL. Technical aspects of the parkes error grid. *Journal of Diabetes Science and Technology*. 2013;7(5):1275-1281.
 43. Bland M. An introduction to medical statistics. 3rd ed. Oxford: Oxford University Press; 2000.
 44. Bland JM, Altman DG. Measuring agreement in method comparison studies. *Statistical Methods in Medical Research*. 1999;8:135-160.
 45. Bland JM, Altman DG. Statistical method for assessing agreement between two methods of clinical measurement. *The Lancet*. 1986;307:310.
 46. Klonoff David C, Lias Courtney, Vigersky Robert, Clarke William, Parkes Joan Lee, Sacks David B, Kirkman M Sue, Kovatchev Boris, the Error Grid Panel. The surveillance error grid. *Journal of Diabetes Science and Technology*. 2014;1–15.
 47. Amir Orna, Weinstein Daphna, Zilberman Silviu, Less Malka, Perl-Treves Daniele, Primack Harel, Weinstein Aharon, Gabis Efi, Fikhte Boris, Karasik Avraham. Continuous noninvasive glucose monitoring technology based on occlusion spectroscopy. *J Diabetes Sci. Technol*. 2007;1(4):463-469.
 48. Wentholt IME, Hart AAM, Hoekstra JBL, Devries JH. How to assess and compare the accuracy of continuous glucose monitors? *Diabetes Technology & Therapeutics*. 2008;10(2):57-68.
 49. Bockle S, Rovati L, Ansari RR. Polarimetric glucose sensing using the Brewster-reflection off-eye lens: Theoretical analysis. *Proc. SPIE*. 2002;4624:160–164.
 50. Boehm Harman-I, Gal A, Raykhman AM, Zahn JD, Naidis E, Mayzel Y. Noninvasive glucose monitoring: A novel approach. *J Diabetes Sci Technol*. 2009;3(2):253–260.
 51. Boehm Harman-I, Gal A, Raykhman AM, Naidis E, Mayzel Y. Noninvasive glucose monitoring: Increasing accuracy by combination of multi-technology and multi-sensors. *J Diabetes Sci Technol*. 2010;4(3):583-595.
 52. Oliver NS, Toumazou C, Cass AEG, Johnston DG. Glucose sensors: A review of current and emerging technology. *Diabetic Medicine*. 2009;26:197–210.
 53. Caduff A, Mueller M, Megej A, Dewarrat F, Suri RE, Klisic J, Donath M, Zakharov P, Schaub D, Stahel WA, Talary Mark S. Characteristics of a multisensor system for non invasive glucose monitoring with external validation and prospective evaluation. *Biosensors and Bioelectronics*. 2011;26:3794–3800.
 54. Caduff A, Dewarrat F, Talary M. Non-invasive glucose monitoring in patients with diabetes: A novel system based on impedance spectroscopy. *Biosens Bioelectron*. 2006;22:598-604.
 55. Caduff A, Hirt E, Feldman Y, Ali Z, Heinemann L. First human experiments with a novel non-invasive, non-optical continuous glucose monitoring system. *Biosens Bioelectron*. 2003;19(3):209–217.
 56. Caduff A, Talary MS, Mueller M. Non-invasive glucose monitoring in patients with Type 1 diabetes: A multisensor system combining sensors for dielectric and optical characterisation of skin. *Biosens Bioelectron*. 2009;24(9):2778–2784.
 57. Enejder AMK, Scecina TG, Oh J, Hunter M, Shih WC, Sasic S, Horowitz GL, Feld MS. Raman spectroscopy for noninvasive glucose measurements. *J. Biomed. Opt*. 2005;10(3):031114.
 58. Lipson J, Bernhardt J, Block U, Freeman WR, Hofmeister R, Hristakeva MBS, Lenosky T, McNamara R, Petrasek D, Veltkamp D, Waydo S. Requirements for calibration in noninvasive glucose monitoring by raman spectroscopy. *Journal of Diabetes Science and Technology*. 2009;3(2):233-241.
 59. Malchoff CD, Shoukri K, Landau JI, Buchert JM. A novel noninvasive blood glucose monitor. *Diabetes Care*. 2002;25:2268-2275.
 60. Myllyla Risto, Zhao Zuomin, Kinnunen Matti. Pulsed photoacoustic techniques and glucose determination in human blood and tissue. Chapter 14, Valery V. Tuchin (Editor), *Handbook of Optical Sensing of Glucose in Biological Fluids and Tissues*, CRC Press, Taylor & Francis Group, 6000

- Broken Sound Parkway NW, Suite 300 Boca Raton, FL 33487-2742. 2009;419-455.
61. Ozaki Y, Shinzawa H, Maruo K. *In vivo* non destructive measurement of blood glucose by near-infrared diffuse-reflectance spectroscopy. Chapter 8, Valery V. Tuchin (Editor), Handbook of Optical Sensing of Glucose in Biological Fluids and Tissues, CRC Press, Taylor & Francis Group, 6000 Broken Sound Parkway NW, Suite 300 Boca Raton, FL 33487-2742. 2009;419-455.
 62. Oliver NS, Toumazou C, Cass AEG, Johnston DG. Glucose sensors: A review of current and emerging technology. *Diabetic Medicine*. 2009;26:197–210.
 63. Pai PP, Sanki PK, Satyabrata S, Banerjee S. Modelling, verification, and calibration of a photo acoustics based continuous noninvasive blood glucose monitoring system. *Review of Scientific Instruments*. 2015;86:064901.
 64. Ramchandani N, Heptulla AR. New technologies for diabetes: A review of the present and the future. *International Journal of Pediatric Endocrinology*. 2012;28:1-10.
 65. Robinson MR, Eaton RP, Haaland DM, Koeppe GW, Thomas EV, Stallard BR, Robinson PL. Noninvasive glucose monitoring in diabetic patients: A preliminary evaluation. *Clin Chem*. 1992; 38:1618-1622.
 66. Tamada JA, Garg S, Jovanovic L. Noninvasive glucose monitoring: comprehensive clinical results. Cygnus Research Team. *JAMA*. 1999;282:1839-1844.
 67. Vaddiraju S, Diane J Burgess, Loannis Tomazos, Faquir C Jain, Fotios P. Technologies for continuous glucose monitoring: Current problems and future promises. *J Diabetes Sci Technol*. 2010;4(6):1540-62.
 68. Valgimigli F, Lucarelli F, Scuffi C, Morandi S, Sposato I. Evaluating the clinical accuracy of GlucoMen® Day: A novel microdialysis-based continuous glucose monitor. *Journal of Diabetes Science and Technology*. 2010;4(5):1182-1192.
 69. Vashist Sandeep Kumar. Non-invasive glucose monitoring technology in diabetes management: A review. *Analytica Chimica Acta*. 2012;750:16–27.
 70. Weiss R, Yegorchikov Y, Shusterman A, Raz I. Noninvasive continuous glucose monitoring using Photoacoustic technology: Results from the first 62 subjects. *Diabetes Technol Ther*. 2007;9:68-74.
 71. Zeng L. Design of a portable noninvasive photoacoustic glucose monitoring system integrated laser diode excitation with annular array detection. *Proceeding of SPIE, Seventh International Conference on Photonics and Imaging in Biology and Medicine*. 2009;7280:72802f-1-72802f-8.
 72. Yoon Gilwon. Statistical analysis for glucose prediction in blood samples by infrared spectroscopy, Chapter 4, Valery V. Tuchin (Editor), Handbook of Optical Sensing of Glucose in Biological Fluids and Tissues, CRC Press, Taylor & Francis Group, 6000 Broken Sound Parkway NW, Suite 300 Boca Raton, FL 33487-2742. 2009;97-114.
 73. Zhao Z, Myllyl R. Photoacoustic blood glucose and skin measurement based on optical scattering effect. *Proc. SPIE*. 2002;4707:153–157.
 74. Myllyla R, Zhao Z, Kinnunen M. Pulsed photoacoustic techniques and glucose determination in human blood and tissue. *Handbook of Optical Sensing of Glucose in Biological Fluids and Tissues*. 2008;419-455.
 75. Zhao Z. Pulsed photoacoustic techniques and glucose determination in human blood and tissue. *Doctoral Thesis, University of Oulu, Finland*; 2002.
 76. Zilberman S, Kononenko A, Weinstein A, Gabis E, Karasin A. Improved system for noninvasive glucose monitoring at home, EASD poster, 932; 2009.

© 2016 Srivastava et al.; This is an Open Access article distributed under the terms of the Creative Commons Attribution License (<http://creativecommons.org/licenses/by/4.0>), which permits unrestricted use, distribution and reproduction in any medium, provided the original work is properly cited.

Peer-review history:
 The peer review history for this paper can be accessed here:
<http://sciencedomain.org/review-history/13975>